

Tangent stiffness method for biaxial bending of reinforced concrete columns

Autor(en): **Chen, W.F. / Shoraka, M.T.**

Objektyp: **Article**

Zeitschrift: **IABSE publications = Mémoires AIPC = IVBH Abhandlungen**

Band (Jahr): **35 (1975)**

PDF erstellt am: **09.07.2024**

Persistenter Link: <https://doi.org/10.5169/seals-26930>

Nutzungsbedingungen

Die ETH-Bibliothek ist Anbieterin der digitalisierten Zeitschriften. Sie besitzt keine Urheberrechte an den Inhalten der Zeitschriften. Die Rechte liegen in der Regel bei den Herausgebern.

Die auf der Plattform e-periodica veröffentlichten Dokumente stehen für nicht-kommerzielle Zwecke in Lehre und Forschung sowie für die private Nutzung frei zur Verfügung. Einzelne Dateien oder Ausdrucke aus diesem Angebot können zusammen mit diesen Nutzungsbedingungen und den korrekten Herkunftsbezeichnungen weitergegeben werden.

Das Veröffentlichen von Bildern in Print- und Online-Publikationen ist nur mit vorheriger Genehmigung der Rechteinhaber erlaubt. Die systematische Speicherung von Teilen des elektronischen Angebots auf anderen Servern bedarf ebenfalls des schriftlichen Einverständnisses der Rechteinhaber.

Haftungsausschluss

Alle Angaben erfolgen ohne Gewähr für Vollständigkeit oder Richtigkeit. Es wird keine Haftung übernommen für Schäden durch die Verwendung von Informationen aus diesem Online-Angebot oder durch das Fehlen von Informationen. Dies gilt auch für Inhalte Dritter, die über dieses Angebot zugänglich sind.

Tangent Stiffness Method for Biaxial Bending of Reinforced Concrete Columns

Méthode tangente de raidissement pour la flexion biaxiale de colonnes en béton armé

Tangent Steifigkeitsmethode zur biaxialen Biegung von Stahlbetonstützen

W.F. CHEN

Assoc. Prof., Dept. of Civil Engrg., Lehigh
University, Bethlehem, Pa.

M.T. SHORAKA

Grad. Student, Dept. of Civil Engrg., Lehigh
University, Bethlehem, Pa.; Formerly Engineer,
Nava Construction Co., Teheran, Iran

Introduction

Moment-curvature-thrust relationships are of prime importance in the analysis of reinforced concrete columns. For a biaxially loaded columns, the appropriate loadings are bending moments M_x and M_y and axial force P . The corresponding deformations are bending curvatures ϕ_x and ϕ_y and axial strain ϵ_o at corner 0. The positive directions of force and deformation vectors are shown in Fig. 1a. For convenience in further discussion, the following vectors of force and deformation are defined;

$$\{F\} = \begin{Bmatrix} M_x \\ M_y \\ P \end{Bmatrix} \quad \{D\} = \begin{Bmatrix} \phi_x \\ \phi_y \\ \epsilon_o \end{Bmatrix} \quad (1)$$

Herein a study is made of the relationship of the force vector $\{F\}$ with the deformation vector $\{D\}$ for a reinforced concrete column segment in biaxial bending.

The non-linear stress-strain relationship in compression as well as the low strength in tension of concrete complicate the analysis of structures using such a material. Hence it is useful to establish an analytical relationship of the force deformation equation in terms of the infinitesimal changes $\{\delta F\}$ and $\{\delta D\}$. This leads to an assumed linear relationship between these vectors.

$$\{\delta F\} = [Q] \{\delta D\} \quad (2)$$

The matrix $[Q]$ is defined as the tangent stiffness matrix as it represents the tangent of the force-deformation curve as well as the stiffness of the cross section.

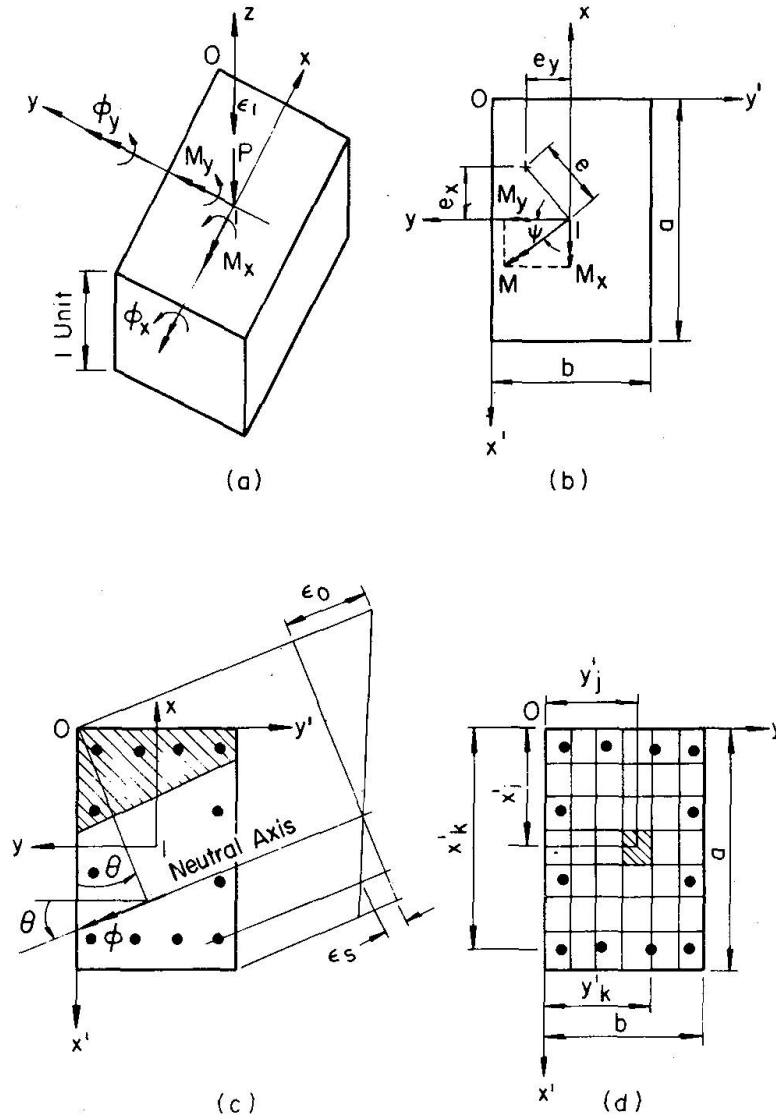


Fig. 1. Moment, Curvature and Strain in Cross Section and Partitioning of Cross Section.

Once this linear relationship is established, it is easy to answer the following three questions:

1. For a given path of force $\{F\}$, the corresponding path of deformation $\{D\}$ can be obtained by step-by-step calculations using Eq. 2, in the form

$$\{\delta D\} = [Q]^{-1} \{\delta F\} \quad (3)$$

and by applying the tangent stiffness method developed in Ref. [1] (Fig. 1 b) for numerical solutions.

2. For a given path of deformation $\{D\}$, the corresponding path of force $\{F\}$ can be obtained by direct step-by-step application of this linear relation, Eq. 2 (Fig. 1 c).
3. This incremental equation (Eq. 2) can also handle any mixed path of force and deformation. For example, the column may be first loaded axially to some

value; and then, holding the axial force P constant, the bending curvatures ϕ_x and ϕ_y may be increased proportionally in magnitude from zero. The corresponding bending moments M_x , M_y and the axial strain ϵ_o can then be obtained by simply subdividing the stiffness matrix $[Q]$ into submatrices. Thus,

$$\begin{Bmatrix} \delta M_x \\ \delta M_y \\ \delta P \end{Bmatrix} = \begin{bmatrix} Q_{11} & Q_{12} & Q_{13} \\ Q_{21} & Q_{22} & Q_{23} \\ Q_{31} & Q_{32} & Q_{33} \end{bmatrix} \begin{Bmatrix} \delta \phi_x \\ \delta \phi_y \\ \delta \epsilon_o \end{Bmatrix} \quad (4)$$

Since $\{\delta P\} = 0$, and $\delta \phi_x$ and $\delta \phi_y$ are known,

$$\delta \epsilon_o = \frac{-1}{Q_{33}} \{Q_{31} \ Q_{32}\} \begin{Bmatrix} \delta \phi_x \\ \delta \phi_y \end{Bmatrix} \quad (5)$$

and

$$\begin{Bmatrix} \delta M_x \\ \delta M_y \end{Bmatrix} = \begin{bmatrix} Q_{11} & Q_{12} & Q_{13} \\ Q_{21} & Q_{22} & Q_{23} \end{bmatrix} \begin{Bmatrix} \delta \phi_x \\ \delta \phi_y \\ \delta \epsilon_o \end{Bmatrix} \quad (6)$$

A somewhat similar solution for this particular mixed path of force and deformations has recently been reported by WARNER [2]. Based upon the equations formulated, a computer program has been developed to provide various numerical results. The elements of the tangent stiffness matrix were evaluated numerically by dividing the concrete section into finite elements and by considering each steel bar as an element (Fig. 1 d).

Assumptions

The procedure is based on the following assumptions.

1. Concrete has no tensile strength, Fig. 2a, and in the usual notation

$$\bar{f}_c = \frac{f_c}{k_1 f_c} = 0 \text{ when } \bar{\epsilon}_c = \frac{\epsilon_c}{\epsilon'_c} \leq 0 \quad (7)$$

2. The stress-strain relationship for concrete in compression is nonlinear and is of the form as shown in Fig. 2a

$$\bar{f}_c = \gamma_1 \bar{\epsilon}_c + (3 - 2\gamma_1) \bar{\epsilon}_c^2 + (\gamma_1 - 2) \bar{\epsilon}_c^3 \text{ when } 0 \leq \bar{\epsilon}_c \leq 1 \quad (8a)$$

$$\bar{f}_c = 1 - \frac{1 - 2\bar{\epsilon}_c + \bar{\epsilon}_c^2}{1 - 2\gamma_2 + \gamma_2^2} \text{ when } 1 \leq \bar{\epsilon}_c \leq \gamma_2 \quad (8b)$$

$$\bar{f}_c = 0 \text{ when } \bar{\epsilon}_c \geq \gamma_2 \quad (8c)$$

where

$$\gamma_1 = \frac{E_c \epsilon'_c}{k_1 f_c} \quad (8d)$$

and γ_2 represents the point of intersection of the stress-strain curve with the strain axis.

3. The stress-strain relationship for steel is elastic perfectly plastic in both tension and compression (Fig. 2b), and in the usual notation

$$\bar{f}_s = \frac{f_s}{f_y} = -1 \quad \text{when } \bar{\epsilon}_s = \frac{\epsilon_s}{\epsilon_y} < -1 \quad (9a)$$

$$\bar{f}_s = \bar{\epsilon}_s \quad \text{when } -1 \leq \bar{\epsilon}_s \leq 1 \quad (9b)$$

$$\bar{f}_s = 1 \quad \text{when } \bar{\epsilon}_s > 1 \quad (9c)$$

4. The effects of creep and shrinkage of the concrete are disregarded.
5. Plane sections remain plane before and after bending.

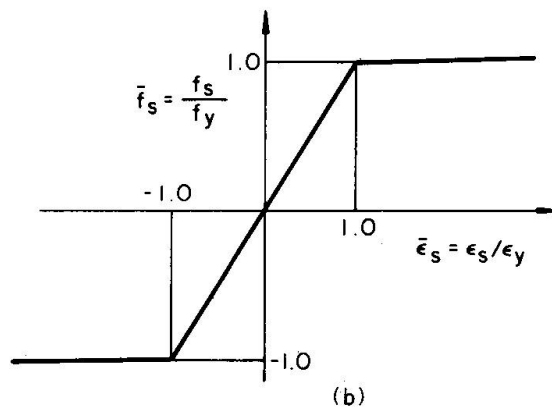
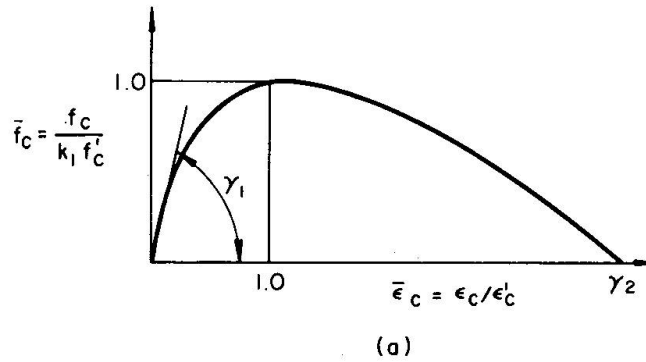


Fig. 2. Stress-Strain Relations.

Formulation of the Basic Equation

Consider the partially yielded cross section shown in Fig. 1c. Equilibrium is satisfied when the internal forces equal the external forces. In x - y coordinate system,

$$M_x = \int \sigma y dA \quad (10a)$$

$$M_y = \int \sigma x dA \quad (10b)$$

$$P = \int \sigma dA \quad (10c)$$

in x' - y' coordinate system,

$$M_{x'} = - \int \sigma y' dA \quad (11a)$$

$$M_{y'} = - \int \sigma x' dA \quad (11b)$$

$$P = \int \sigma dA \quad (11c)$$

In order to evaluate the internal actions, the concrete area is divided by horizontal and vertical lines into a total of N_c small rectangular elements, ΔA_c (Fig. 1d). The total steel area is assumed to be distributed in N_s elements, all of equal area ΔA_s . The relation between ΔA_s and ΔA_c is

$$\Delta A_s = p' \Delta A_c \quad (12)$$

where

$$p' = \frac{N_c}{N_s} p, \quad p = \frac{A_s}{ab} \quad (13)$$

and Eq. 11 may be rewritten in the form (Fig. 1d)

$$M_{x'} = - \left\{ \sum_{i=1}^{N_a} \sum_{j=1}^{N_b} y'_j (f_c)_{ij} + p' \sum_{k=1}^{N_s} y'_k (f_s)_k - p' \sum_{k=1}^{N_s} y'_k (f_c)_k \right\} \Delta A_c \quad (14)$$

$$M_{y'} = - \left\{ \sum_{i=1}^{N_a} \sum_{j=1}^{N_b} x'_i (f_c)_{ij} + p' \sum_{k=1}^{N_s} x'_k (f_s)_k - p' \sum_{k=1}^{N_s} x'_k (f_c)_k \right\} \Delta A_c \quad (14b)$$

$$P = \left\{ \sum_{i=1}^{N_a} \sum_{j=1}^{N_b} (f_c)_{ij} + p' \sum_{k=1}^{N_s} (f_s)_k - p' \sum_{k=1}^{N_s} (f_c)_k \right\} \Delta A_c \quad (14c)$$

where N_a and N_b are the numbers of rows and columns of elemental concrete areas respectively, and N_s is the number of bars.

The incremental forms of the equilibrium equations are

$$\delta M_{x'} = - \left\{ \sum_{i=1}^{N_a} \sum_{j=1}^{N_b} y'_j (\delta f_c)_{ij} + p' \sum_{k=1}^{N_s} y'_k (\delta f_s)_k - p' \sum_{k=1}^{N_s} y'_k (\delta f_c)_k \right\} \Delta A_c \quad (15a)$$

$$\delta M_{y'} = - \left\{ \sum_{i=1}^{N_a} \sum_{j=1}^{N_b} x'_i (\delta f_c)_{ij} + p' \sum_{k=1}^{N_s} x'_k (\delta f_s)_k - p' \sum_{k=1}^{N_s} x'_k (\delta f_c)_k \right\} \Delta A_c \quad (15b)$$

$$\delta P = \left\{ \sum_{i=1}^{N_a} \sum_{j=1}^{N_b} (\delta f_c)_{ij} + p' \sum_{k=1}^{N_s} (\delta f_s)_k - p' \sum_{k=1}^{N_s} (\delta f_c)_k \right\} \Delta A_c \quad (15c)$$

The incremental changes of stress and strain in concrete are related by

$$\delta f_c = G_c \delta \epsilon_c \quad (16)$$

where

$$G_c = 0, \text{ when } \epsilon_c \leq 0 \quad (17a)$$

$$G_c = \frac{k_1 f'_c}{\epsilon'_c} \gamma_1 + 2 \frac{k_1 f'_c}{\epsilon'^2_c} (3 - 2\gamma_1) \epsilon_c + 3 \frac{k_1 f'_c}{\epsilon'^3_c} (\gamma_1 - 2) \epsilon_c^2 \quad (17b)$$

when

$$0 < \varepsilon_c \leq \varepsilon'_c$$

and

$$G_c = 2 \frac{k_1 f'_c}{\varepsilon'_c (1 - 2\gamma_2 + \gamma_2^2)} - 2 \frac{k_1 f'_c}{\varepsilon_c'^2 (1 - 2\gamma_2 + \gamma_2^2)} \varepsilon_c \quad (17c)$$

when

$$\varepsilon'_c < \varepsilon_c \leq \varepsilon'_c \gamma_2$$

and

$$G_c = 0, \text{ when } \varepsilon_c > \varepsilon'_c \gamma_2 \quad (17d)$$

The incremental changes in stress and strain of steel are related by

$$\delta f_s = G_s \delta \varepsilon_s \quad (18)$$

where

$$G_s = 0, \text{ when } \varepsilon_s < -\varepsilon_y \quad (19a)$$

and

$$G_s = \frac{f_y}{\varepsilon_y} = E_s, \text{ when } -\varepsilon_y \leq \varepsilon_s \leq \varepsilon_y \quad (19b)$$

and

$$G_s = 0, \text{ when } \varepsilon_s > \varepsilon_y \quad (19c)$$

Substituting δf_c and δf_s from equations 16 and 18 into equation 15, we have,

$$\begin{aligned} \delta M_{x'} = & - \left\{ \sum_{i=1}^{N_a} \sum_{j=1}^{N_b} y'_j (G_c)_{ij} (\delta \varepsilon_c)_{ij} + p' \sum_{k=1}^{N_s} y'_k (G_s)_k (\delta \varepsilon_s)_k - \right. \\ & \left. p' \sum_{k=1}^{N_s} y'_k (G_c)_k (\delta \varepsilon_c)_k \right\} \Delta A_c \end{aligned} \quad (20a)$$

$$\begin{aligned} \delta M_{y'} = & - \left\{ \sum_{i=1}^{N_a} \sum_{j=1}^{N_b} x'_i (G_c)_{ij} (\delta \varepsilon_c)_{ij} + p' \sum_{k=1}^{N_s} x'_k (G_s)_k (\delta \varepsilon_s)_k - \right. \\ & \left. p' \sum_{k=1}^{N_s} x'_k (G_c)_k (\delta \varepsilon_c)_k \right\} \Delta A_c \end{aligned} \quad (20b)$$

$$\delta P = \left\{ \sum_{i=1}^{N_a} \sum_{j=1}^{N_b} (G_c)_{ij} (\delta \varepsilon_c)_{ij} + p' \sum_{k=1}^{N_s} (G_s)_k (\delta \varepsilon_s)_k - p' \sum_{k=1}^{N_s} (G_c)_k (\delta \varepsilon_c)_k \right\} \Delta A_c \quad (20c)$$

The strain ε at any point in the cross section with respect to $x'y'$ coordinate can be expressed in a linear form as

$$\varepsilon = -y' \varphi_{x'} - x' \varphi_{y'} + \varepsilon_o \quad (21)$$

where ε_o is the strain at the corner 0 (Fig. 1). The incremental change of the strain is

$$\delta \varepsilon = -y' \delta \varphi_{x'} - x' \delta \varphi_{y'} + \delta \varepsilon_o \quad (22)$$

or (Fig. 1d)

$$(\delta \varepsilon_c)_{ij} = -y'_j \delta \varphi_{x'} - x'_i \delta \varphi_{y'} + \delta \varepsilon_o \quad (23a)$$

$$(\delta \varepsilon_s)_k = (\delta \varepsilon_c)_k = -y'_k \delta \varphi_{x'} - x'_k \delta \varphi_{y'} + \delta \varepsilon_o \quad (23b)$$

where $\delta\epsilon_0$ is the strain increment at the corner 0 of the cross section. Combinations of equations 20 and 23 gives a set of simultaneous linear equations which can be written in the matrix form as

$$\begin{Bmatrix} \delta M_{x'} \\ \delta M_{y'} \\ \delta P \end{Bmatrix} = \begin{bmatrix} Q_{11} & Q_{12} & Q_{13} \\ Q_{21} & Q_{22} & Q_{23} \\ Q_{31} & Q_{32} & Q_{33} \end{bmatrix} \begin{Bmatrix} \delta\phi_{x'} \\ \delta\phi_{y'} \\ \delta\epsilon_0 \end{Bmatrix} \quad (24)$$

where Q_{ij} is defined as

$$Q_{11} = \left\{ \sum_{i=1}^{N_a} \sum_{j=1}^{N_b} (y'_j)^2 (G_c)_{ij} + p' \sum_{k=1}^{N_s} (y'_k)^2 (G_s)_k - p' \sum_{k=1}^{N_s} (y'_k)^2 (G_c)_k \right\} \Delta A_c \quad (25a)$$

$$Q_{22} = \left\{ \sum_{i=1}^{N_a} \sum_{j=1}^{N_b} (x'_i)^2 (G_c)_{ij} + p' \sum_{k=1}^{N_s} (x'_k)^2 (G_s)_k - p' \sum_{k=1}^{N_s} (x'_k)^2 (G_c)_k \right\} \Delta A_c \quad (25b)$$

$$Q_{33} = \left\{ \sum_{i=1}^{N_a} \sum_{j=1}^{N_b} (G_c)_{ij} + p' \sum_{k=1}^{N_s} (G_s)_k - p' \sum_{k=1}^{N_s} (G_c)_k \right\} \Delta A_c \quad (25c)$$

$$Q_{12} = Q_{21} = \left\{ \sum_{i=1}^{N_a} \sum_{j=1}^{N_b} x'_i y'_j (G_c)_{ij} + p' \sum_{k=1}^{N_s} x'_k y'_k (G_s)_k - p' \sum_{k=1}^{N_s} x'_k y'_k (G_c)_k \right\} \Delta A_c \quad (25d)$$

$$Q_{13} = Q_{31} = - \left\{ \sum_{i=1}^{N_a} \sum_{j=1}^{N_b} y'_j (G_c)_{ij} + p' \sum_{k=1}^{N_s} y'_k (G_s)_k - p' \sum_{k=1}^{N_s} y'_k (G_c)_k \right\} \Delta A_c \quad (25e)$$

$$Q_{23} = Q_{32} = - \left\{ \sum_{i=1}^{N_a} \sum_{j=1}^{N_b} x'_i (G_c)_{ij} + p' \sum_{k=1}^{N_s} x'_k (G_s)_k - p' \sum_{k=1}^{N_s} x'_k (G_c)_k \right\} \Delta A_c \quad (25f)$$

Equation 24 can be rewritten as

$$\{\delta F\} = [Q] \{\delta D\} \quad (26)$$

The symmetric matrix $[Q]$, whose elements are given by Equation 25 is known as the tangent stiffness matrix as it represents the tangent of the force-deformation curve as well as the stiffness of the cross section.

Numerical Studies

Based upon the equations formulated, a computer program using the tangent stiffness technique [1] was developed to provide numerical results. The numerical work was performed on a high speed digital computer (CDC 6400). The specific case of a square section with the following input values was treated as a standard concrete column cross section:

$$a = 24 \text{ in, } b = 24 \text{ in, } N_a = 10, N_b = 10$$

$$N_s = 12, p = \frac{A_s}{ab} = 0.0325, k_1 f'_c = 4.2 \text{ ksi}$$

$$k_1 = 0.85, f_s = 60.0 \text{ ksi, } \epsilon'_c = 0.002$$

$$E_s = 29,000,000 \text{ psi, } E_c = 57,600 \sqrt{f'_c} \text{ (for normal weight concrete)}$$

$$\gamma_2 = 4, \gamma_1 = \text{computed from Eq. 8d.}$$

The elements of the tangent stiffness matrix of the cross section were evaluated numerically by dividing the cross section into finite elements N_c (Fig. 1d). The value of N_c was varied from 100 (10×10) to 400 (20×20) for the square section. The increase in accuracy obtained by using the finer grids was only 0.1%. A partitioning of the concrete cross section into 100 elements and the steel areas into 12 elements distributed uniformly around the sides of the section are used herein. A somewhat similar partitioning was also suggested in Ref. 2.

The strain and stress in each element were computed as the average value at its centroid. All force and deformation vectors are nondimensionalized as,

Force vector

$$\left\{ \begin{array}{ccc} P & M_x & M_y \\ f'_c ab & f'_c ab^2 & f'_c a^2 b \end{array} \right\}$$

Deformation vector

$$\left\{ \begin{array}{ccc} \varphi_x & \varphi_y & \varepsilon_o \\ \left(\frac{\varepsilon'_c}{a} \right) & \left(\frac{\varepsilon'_c}{b} \right) & \varepsilon'_c \end{array} \right\}$$

The allowable error in $P/f'_c a b$ was 0.002.

The resultant moment on the section may be represented by the two components M_x and M_y or by a vector M of magnitude $\sqrt{M_x^2 + M_y^2}$ and inclined at the angle $\Psi = \tan^{-1}(M_x/M_y)$ to the y axis (see Fig. 1b). The resultant curvature φ of magnitude $\sqrt{\varphi_x^2 + \varphi_y^2}$ and inclined at the angle $\theta = \tan^{-1}(\varphi_x/\varphi_y)$ to the y axis (Fig. 1c) is nondimensionalized as $\varphi/(\varepsilon'_c/b)$.

Example – Given Path of Loading

The moment-curvature curves plotted in Fig. 3, 4, 6, 7, and 8 are for M_x vs. φ_x for various values of M_y . The column section is first loaded axially up to some value and then bent by M_y to some other value while keeping P constant and finally bent by M_x to failure while keeping P and M_y constant. The curves have been terminated when the strain ratio $\varepsilon_o/\varepsilon'_c$ reaches the value 3.0. To indicate the magnitude of the strains in the cross section, two other lines of constant $\varepsilon_o/\varepsilon'_c =$ recommended by ACI [3] and 2.0 have been plotted across the main curves (dotted lines in the figures).

It is of interest to note that the values of the maximum moment $M_x/f'_c ab^2$ lie between the values of $\varepsilon_o/\varepsilon'_c = 2.0$ to 3.0 and generally very close to the constant line $\varepsilon_o/\varepsilon'_c = 3.0$. The maximum values of the moment are indicated by the small circles in Figures 3 to 8. These moment curvature curves indicate that the maximum strength of short columns in biaxial bending and compression are not unduly sensitive to the variations in the assumed concrete ultimate strain which is often chosen in the range between 0.003 and 0.004.

The moment curvature curves shown in Fig. 3 are considered to be the standard cases. The important factors influencing the behavior of the curves are the magnitude of compression force P , concrete quality $k_1 f'_c$, steel quality f_y , and percentage of

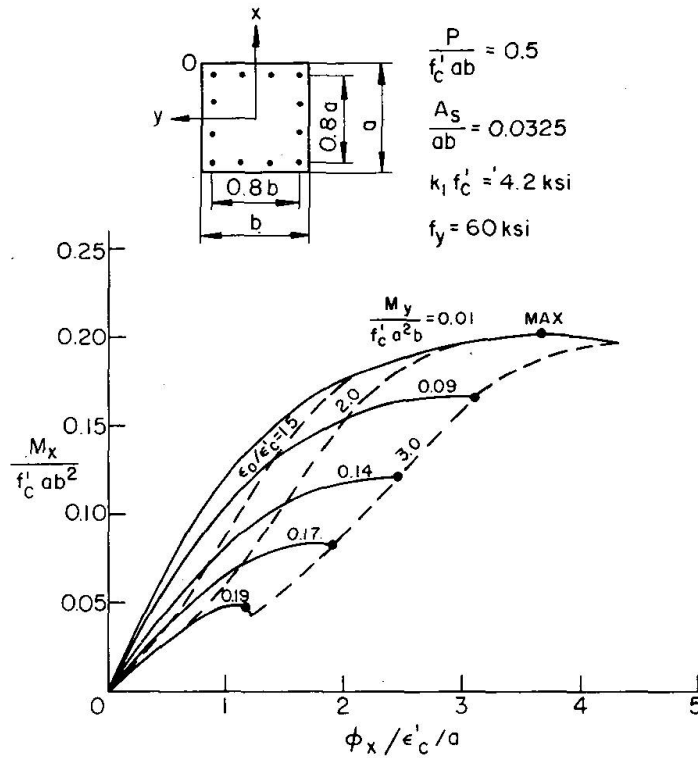


Fig. 3. Moment-Curvature Relations: Standard Case.

reinforcement A_s/ab . The variations of these factors with respect to the standard case are given in Figs. 4, 6, 7, and 8.

The influence of axial compression force on the moment curvature curves is shown in Fig. 4. The unloading of the moment, M_x , with respect to an increase in curvature ϕ_x is not seen for the curves $P = 0.1 f'_c ab$ within the range $\epsilon_o/\epsilon'_c = 3.0$ but is rather rapid for the curves with $P = 1.0 f'_c ab$. It is also observed, that when $P = 1.0 f'_c ab$ and the bending moment $M_y \geq 0.05 f'_c a^2 b$, there is a very rapid unloading for both moment M_x and curvature ϕ_x . The curvature ϕ_y or the resultant curvature ϕ is, of course, not unloaded with respect to a decrease in moment M_x , as shown in Fig. 5.

The influence of concrete quality $k_1 f'_c$ and steel quality f_y on the moment curvature curves is shown in Figs. 6 and 7. The results are calculated for concrete with $k_1 f'_c = 3.0$ ksi and 5.0 ksi (Fig. 6) and for steel with $f_y = 40$ ksi and 80 ksi (Fig. 7) respectively. As can be seen, an increase in material qualities significantly increases the stiffness and strength of a biaxially loaded cross section.

Figure 8 shows the influence of the percentage reinforcement A_s/ab on the moment curvature relationships. It is evident from the figure that the percentage steel reinforcement has an appreciable effect on the behavior of a biaxially loaded cross section.

The maximum points of the moment curvature curves as shown by the small circles in Figs. 3 to 8 represent the maximum strength of the biaxially loaded cross section. The maximum loads obtained in this way for the standard cross section (Fig. 3) with three values of strain ratio, $\epsilon_o/\epsilon'_c = 1.5, 2.0$ and 3.0 are represented by the interaction curves in Figs. 9 to 13. The small circles in these figures indicate

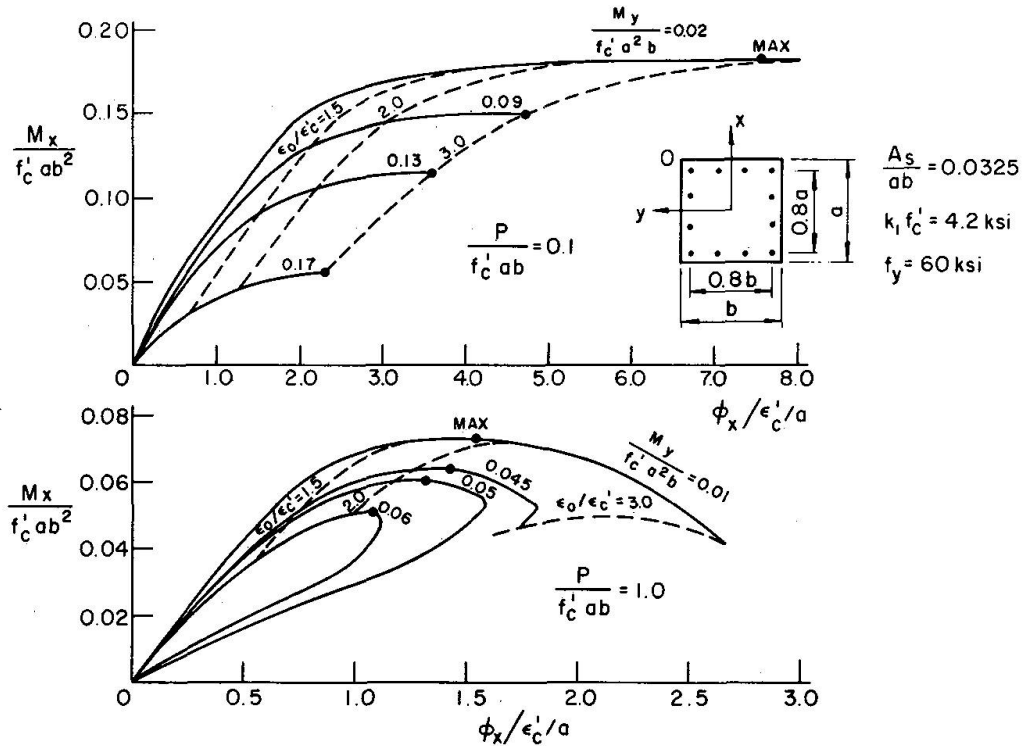


Fig. 4. Moment-Curvature Relations: Axial Compression Force Effect.

the regions where the maximum load is controlled either by the maximum concrete strain or by the overall stress distribution of the cross section. The important factors influencing the maximum carrying capacity of a biaxially loaded short column are the axial compression force, P , the concrete quality, $k_1 f'_c$, steel quality, f_y , and percentage of reinforcement A_s/ab , as shown in Figs. 9 to 13, respectively. Since the interaction curves are nondimensionalized, they can be directly used in analysis and design computations.

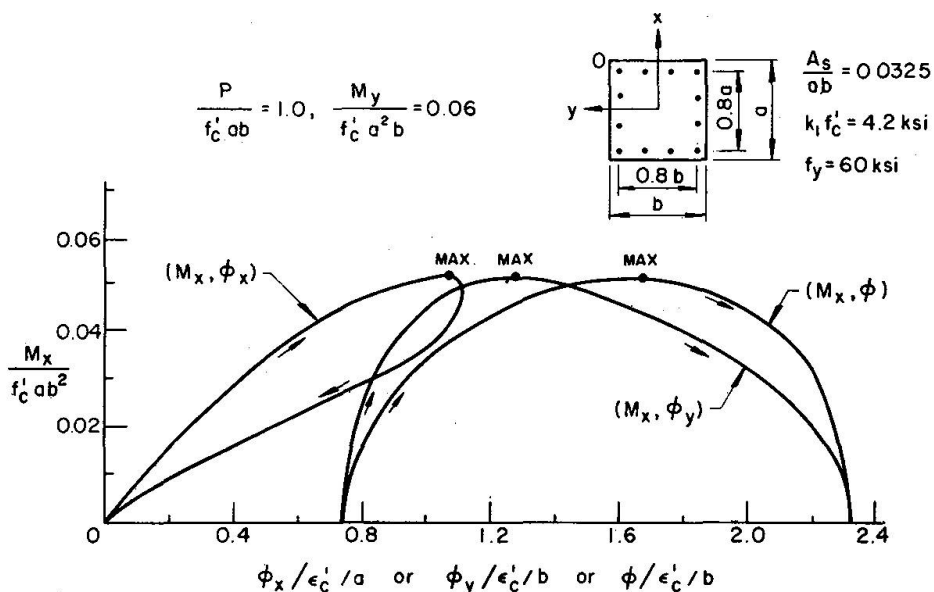


Fig. 5. Moment-Curvature Relations: Complete Unloading.

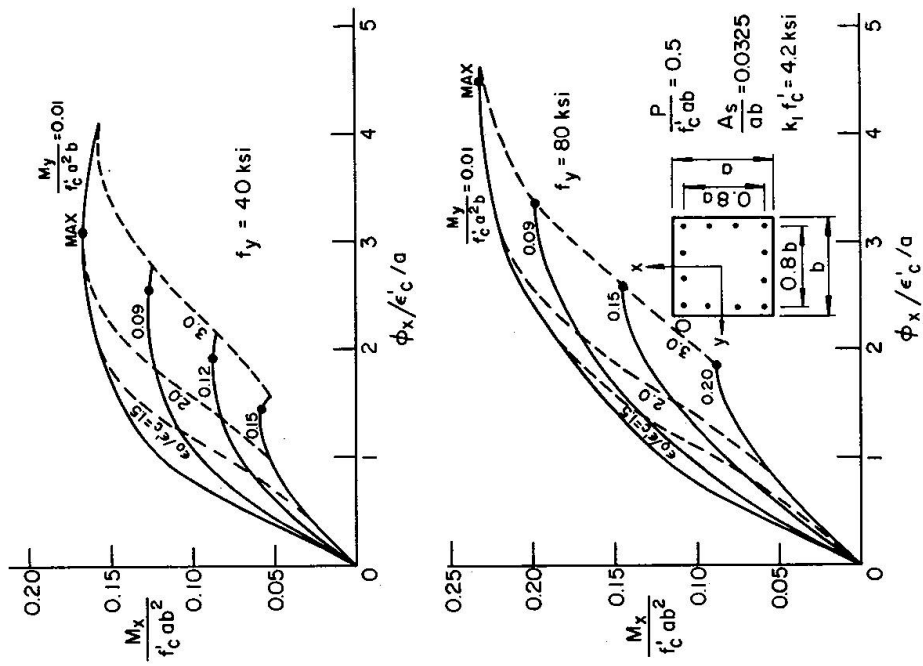


Fig. 6. Moment-Curvature Relations: Concrete Quality Effect.

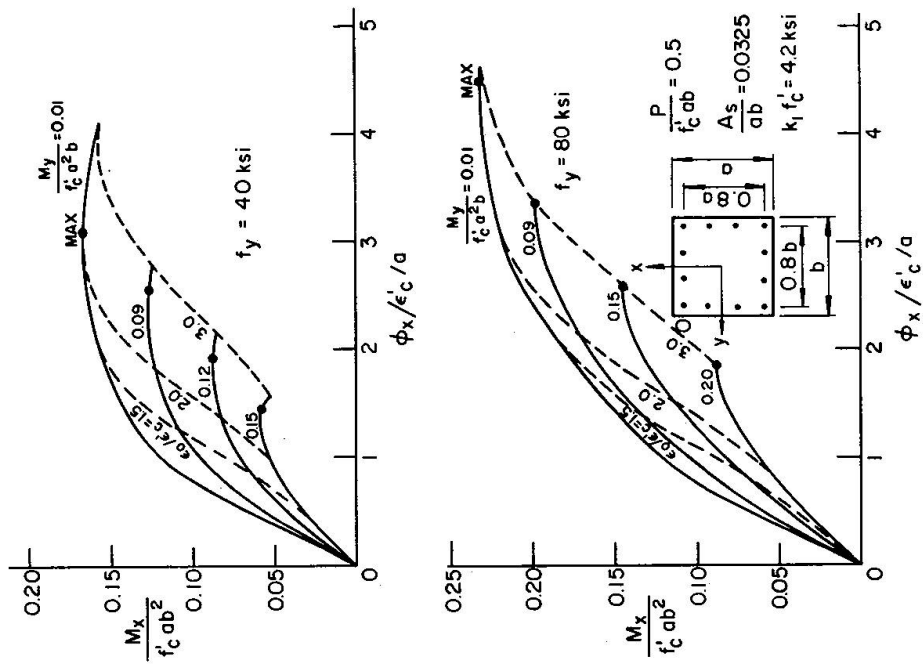


Fig. 7. Moment-Curvature Relations: Steel Quality Effect.

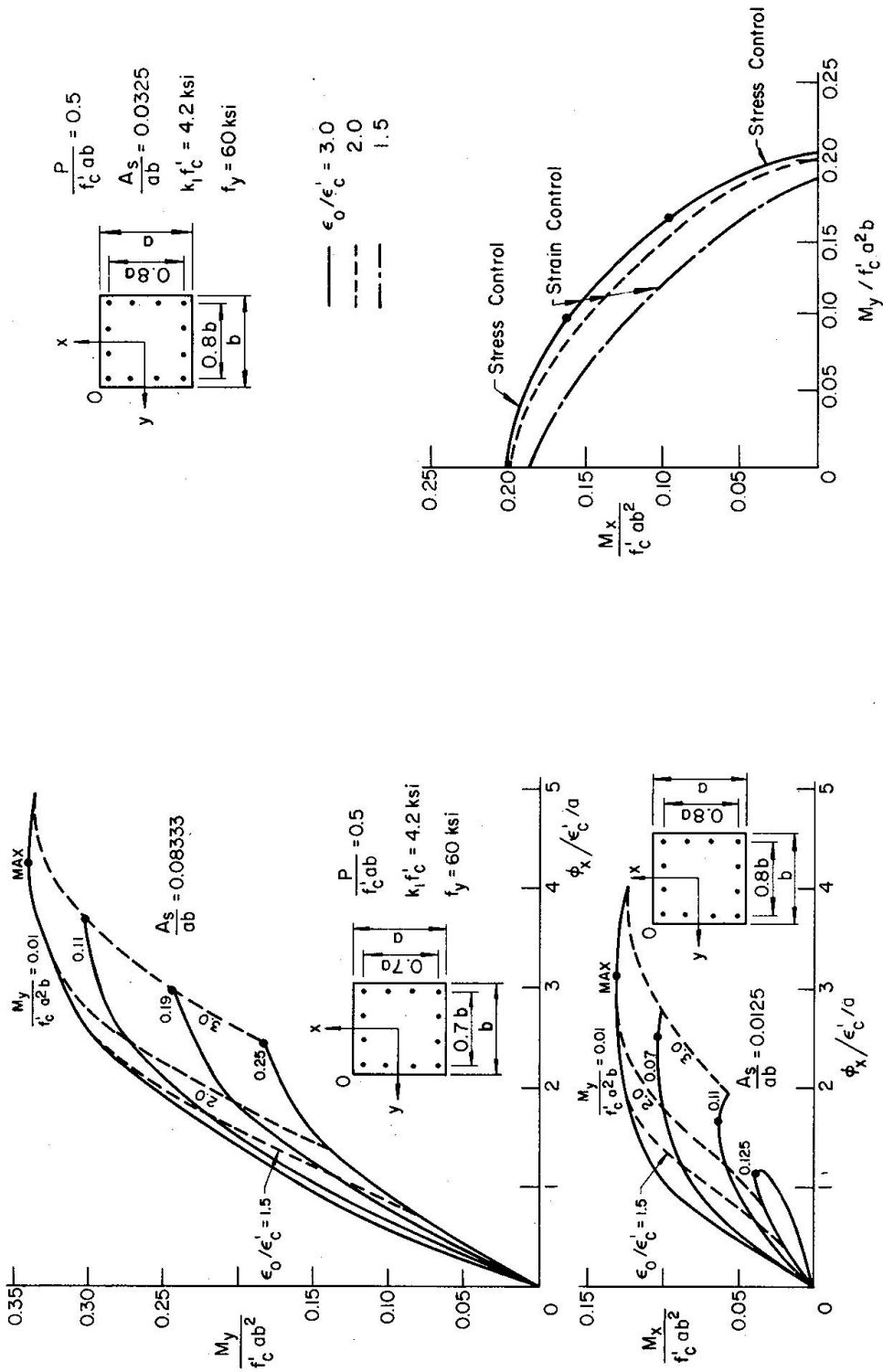


Fig. 8. Moment-Curvature Relations: Percentage of Reinforcement Effect.

Fig. 9. Interaction Curves: Standard Case.

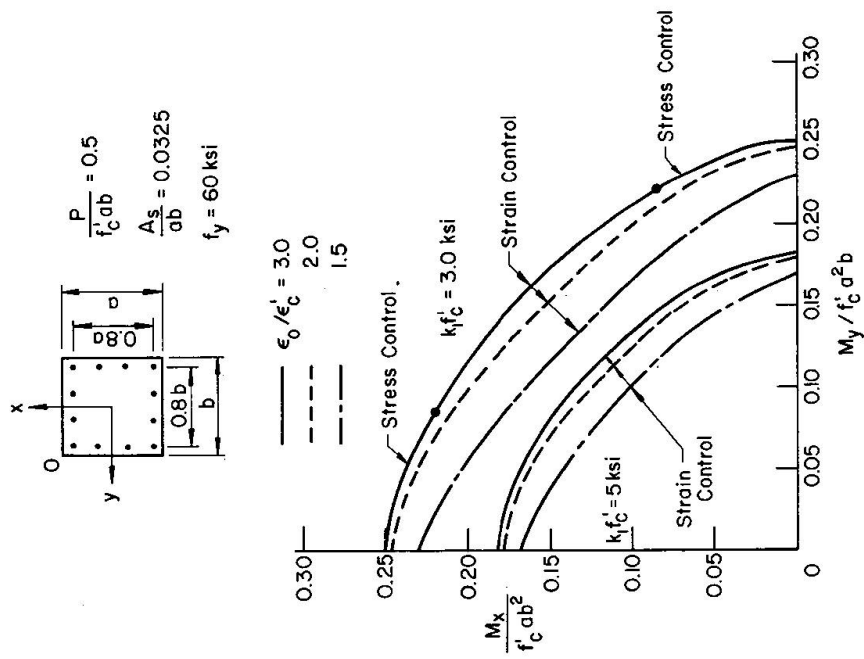


Fig. 11. Interaction Curves: Concrete Quality Effect.

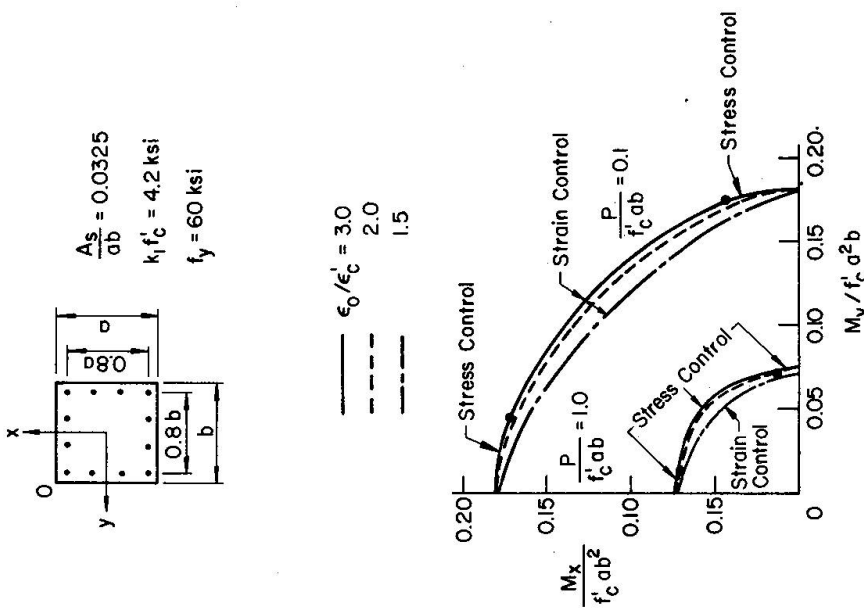


Fig. 10. Interaction Curves: Axial Compression Force Effect.

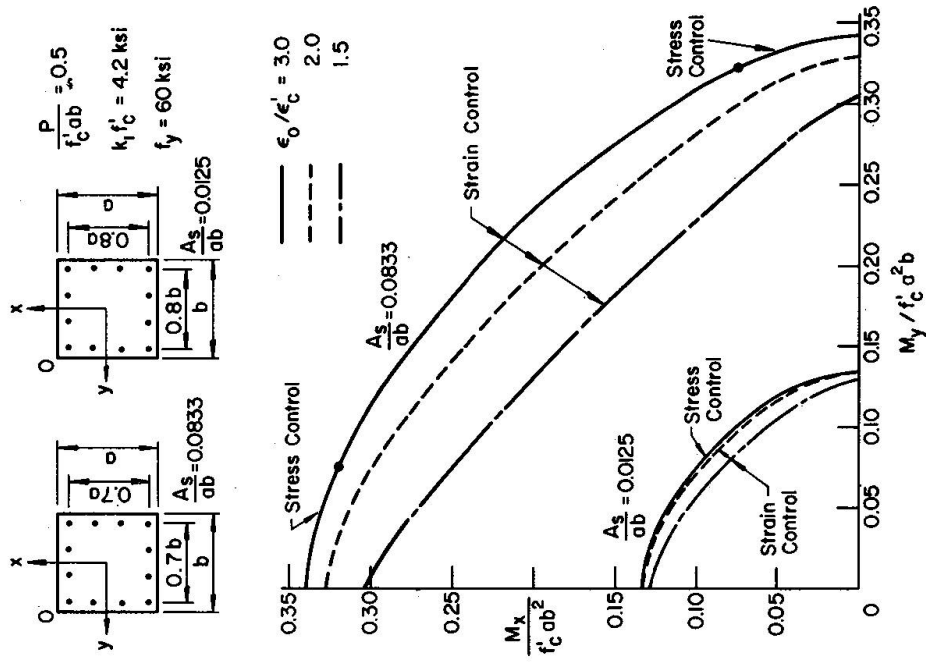


Fig. 13. Interaction Curves: Percentage of Reinforcement Effect.

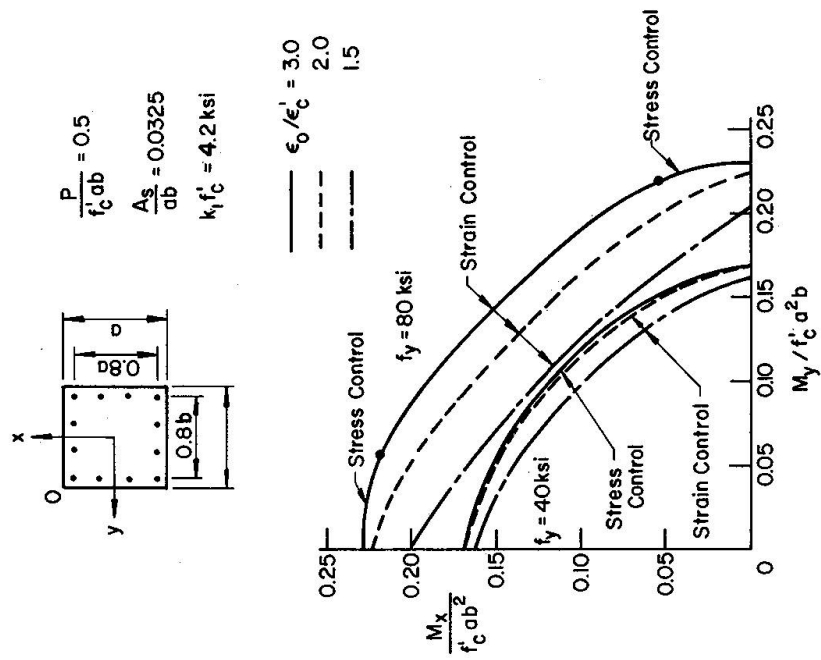


Fig. 12. Interaction Curves: Steel Quality Effect.

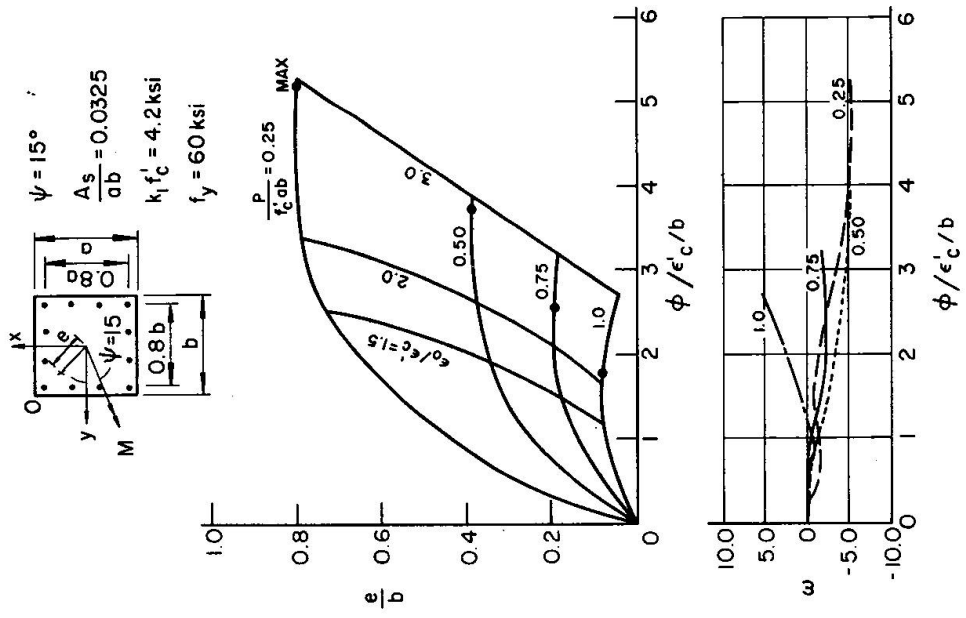


Fig. 15. Moment-Curvature Relations: $\Psi = 15^\circ$.
($\omega = \Psi - \theta$)

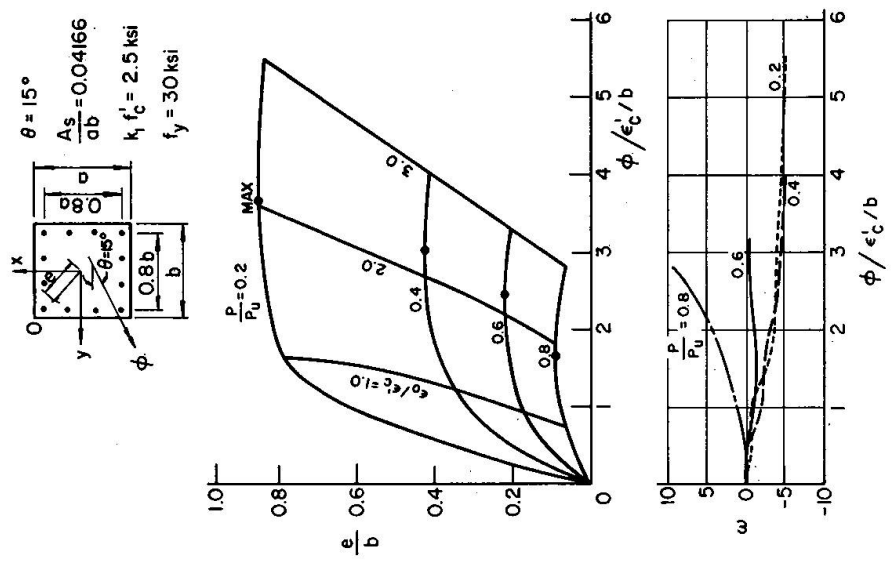


Fig. 14. Moment-Curvature Relations: $\theta = 15^\circ$.
($\omega = \Psi - \theta$)

Example – Given Mixed Path of Loading and Deformation

The moment-curvature curves plotted in Fig. 14 are for e/b vs. ϕ for a given set of values of $\theta = \tan^{-1} (\phi_x/\phi_y) = 15^\circ$ and $P/P_u = 0.2, 0.4, 0.6$ and 0.8 . In the figure, the column section is first loaded axially to some value; and then the axial force P is held constant while the bending curvatures ϕ_x and ϕ_y (or $\phi = \sqrt{\phi_x^2 + \phi_y^2}$) are increased proportionally in magnitude from zero. The corresponding bending moments M_x and M_y (or $e = M/P = \sqrt{M_x^2 + M_y^2}/P$) and axial strain ϵ_o at the corner 0 (Fig. 14) can be obtained by the Eqs. 5 and 6 using the iterative procedure reported in Ref. 2. These moment curvature curves were compared with those obtained previously by Warner and an excellent agreement was found in all cases [2].

The maximum difference between the angles θ and Ψ , i.e. between the directions of the resultant curvature ϕ and resultant moment vectors, $\omega = \Psi - \theta$, is also shown in Fig. 14. It can be seen that the moment and curvature vectors nearly coincide in direction throughout the entire range of loading. The maximum difference between the two vectors is of the order of ten degrees.

It is also of interest to note that a similar conclusion is also true for the case of other loading paths. For example, in Fig. 15, the section is first loaded axially to some constant value and then the axial force P is held constant while the bending moments M_x and M_y are increased proportionally in magnitude; i.e. $\Psi = \tan^{-1} (M_x/M_y)$. The corresponding bending curvatures ϕ_x and ϕ_y and axial strain ϵ_o can be obtained by Eq. 3 using the iterative procedure reported in Ref. 1. The maximum difference between the angles θ and Ψ is again only of the order of ten degrees.

Simple Interaction Equations

The general form of the interaction curves shown in Figs. 9-13 may be approximated by a non-dimensional interaction equation [4]:

$$\left(\frac{M_x}{M_{x0}}\right)^\alpha + \left(\frac{M_y}{M_{y0}}\right)^\alpha = 1.0 \quad (27)$$

where M_{x0} and M_{y0} represent the load carrying capacities of a particular column under compression and uniaxial bending moment about x and y axes, respectively. Thus, for a given compression P , M_{x0} and M_{y0} are the values given on the $M_y = 0$ and $M_x = 0$ axes shown in Figs. 9-13. The value α is the exponent depending on column dimensions, amount and distribution of steel reinforcement, stress-strain characteristics of steel and concrete, and magnitude of axial compression. For a given compression and a given column characteristic, the value of α is a numerical constant.

The interaction surface corresponding to the column section given in Figs. 9 and 10 is shown in Fig. 16a. The interaction curves given previously in Figs. 9 and 10 for the particular case of strain ratio $\epsilon_o/\epsilon'_c = 1.5$ are now non-dimensionalized by the values M_{x0} and M_{y0} and plotted in Fig. 16b. These curves corresponding to constant values of $P/f'_c ab = 0.1, 0.5$ and 1.0 which may be thought of as "load contours".

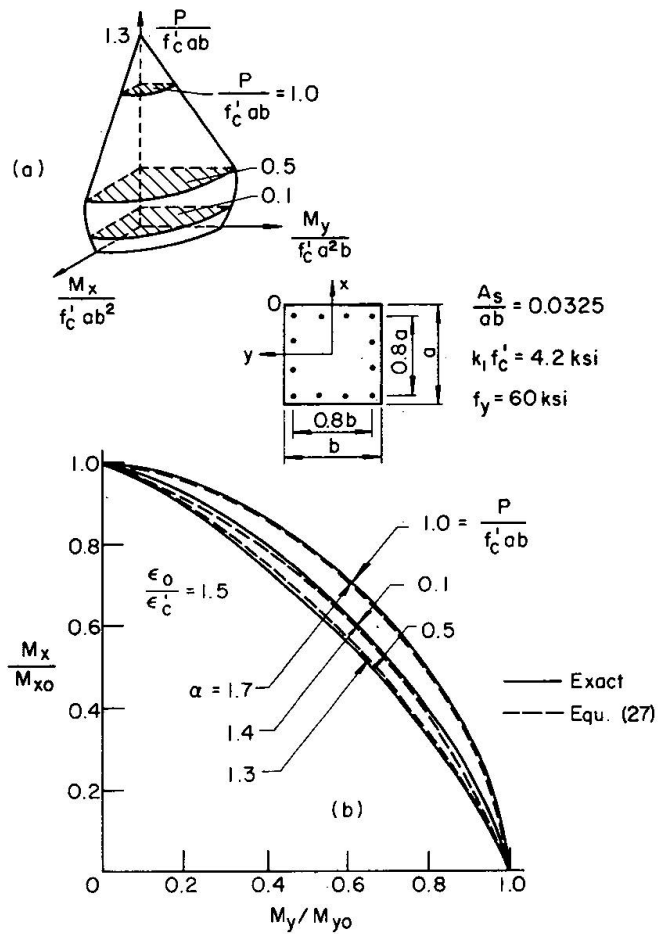


Fig. 16. Comparison of Interaction Curves.

Using Eq. 27, values of α are calculated for this column. The calculated values of α are found, varying from 1.3 to 1.4 for $P/f'_c ab = 0.1$ and 0.5 but jumping to 1.7 for $P/f'_c ab = 1.0$. The comparison between the actual curves computed directly on the basis of stress-strain relations and the theoretical curves obtained from Eq. 27 is also shown in Fig. 16b and good agreement is observed. The values of α for columns with a wide range of variation in values of f'_c , f_y and A_s/ab are tabulated in Table 1 for the particular case of strain ratio $\epsilon_o/\epsilon'_c = 1.5$ (recom-

Table 1. Computed Values of α in Eq. 27

$\frac{P}{f'_c ab}$	$k_1 f'_c$	f_y	$\frac{A_s}{ab}$	α	Note
0.5	4.2	60	0.0325	1.3	$\frac{\epsilon_o}{\epsilon'_c} = 1.5$ for all cases.
0.1	4.2	60	0.0325	1.4	
1.0	4.2	60	0.0325	1.7	
0.5	3	60	0.0325	1.3	
0.5	5	60	0.0325	1.4	
0.5	4.2	40	0.0325	1.4	
0.5	4.2	80	0.0325	1.2	
0.5	4.2	60	0.0125	1.4	
0.5	4.2	60	0.0833	1.1	

mended by ACI). In general, the values of α in the range 1.1 to 1.4 are seen to give a good approximation for all the cases investigated in the low and moderate axial compression range, but large variation in values of α is observed for columns with high axial compression.

Notations

a	depth of section.
b	width of section.
$\{D\}$	$\{\varphi_x \varphi_y \varepsilon_o\}$ = deformation vector.
E_c	modulus of elasticity of concrete.
E_s	modulus of elasticity of steel.
e	$\frac{M}{P}$ = (Fig. 1 b).
$\{F\}$	$\{M_x M_y P\}$ = force vector.
f_c	concrete stress.
f'_c	specified cylinder compression strength of concrete.
$\frac{f_c}{f'_c}$	f_c/f'_c .
f_s	steel stress.
$\frac{f_s}{f_y}$	f_s/f_y .
f_y	specified yield strength of reinforcement.
G_c	$\frac{\delta f_c}{\delta \varepsilon_c}$.
G_s	$\frac{\delta f_s}{\delta \varepsilon_s}$.
k_1	ratio of strength of concrete in member to specified cylinder compression strength.
M	$\sqrt{M_x^2 + M_y^2}$;
$M_x, M_{x'}$	moment with respect to x and x' axes respectively.
M_{xo}, M_{yo}	maximum moment capacity with respect to x and y axes respectively.
$M_y, M_{y'}$	moment with respect to y and y' axes respectively.
N_a	number of rows of elemental concrete areas.
N_b	number of columns of elemental concrete areas.
N_c	$N_a N_b$ = total number of elemental concrete areas.
N_s	number of reinforcement elemental areas.
P	compression force in section.
P_u	failure load of section for zero eccentricity.
p	A_s/ab .
p'	$\frac{N_c}{N_s} p$.
α	defined in Eq. 27.
γ_1	$\frac{E_c \varepsilon'_c}{k_1 f'_c}$.
γ_2	the point of intersection of the stress-strain curve with strain axis (Fig. 2a).
ε	strain.
ε_c	concrete strain.

ε'_c	concrete strain when concrete stress is $k_1 f'_c$.
$\bar{\varepsilon}_c$	$\frac{\varepsilon_c}{\varepsilon'_c}$
ε_o	strain at corner 0.
ε_s	steel strain.
ε_y	steel yield strain.
$\bar{\varepsilon}_s$	$\frac{\varepsilon_s}{\varepsilon_y}$.
θ	inclination of the curvature vector to the y axis.
σ	stress.
ϕ	$\sqrt{\phi_x^2 + \phi_y^2}$.
$\phi_x, \phi_{x'}$	curvature with respect to x and x' axes respectively.
$\phi_y, \phi_{y'}$	curvature with respect to y and y' axes respectively.
Ψ	inclination of moment vector to the y axis. And
ω	$\Psi - \theta$.

Acknowledgments

The research reported here was supported by the National Science Foundation under Grant GK-35886 to Lehigh University.

Key Words

Moments; Biaxial bending; Columns; Plasticity; Reinforced Concrete; Curvature; Computers; Structural Engineering.

Abstract

Analytical formulations and procedures are developed for computing moment-thrust-curvature relations for reinforced concrete column sections in biaxial bending. The cross section is partitioned by a rectangular grid into a large number of small elemental areas of steel and concrete. The moment-thrust-curvature relations are obtained by step-by-step application of the analytically developed linear force-deformation equation using the tangent stiffness iterative procedure. The method is found to be extremely powerful and efficient for computer solution.

Numerical results are obtained for two types of loading paths: (a) given path of loading; and (b) given mixed path of loading and deformation. Results are presented in the form of moment-curvature-thrust curves and interaction curves relating axial compression and biaxial bending moments. The important factors influencing the behavior of these curves are discussed such as strength of materials, percentage of reinforcement and the magnitude of compression force. Simple analytical expressions to approximate the interaction curves of square sections are obtained.

Objective consequences with respect to the security and economy

The elastic-plastic behavior of an isolated, reinforced concrete column subjected to an axial load, and two bending moments acting in two perpendicular directions, is an important technical problem with frequent engineering applications. The obvious example is a corner column in a space building frame. Because the behavior of a space structure is characterized by the behavior of each of its individual members, it is of fundamental importance in the analysis and design of a three-dimensional space structure that we develop basic knowledge of the response of each individual member to forces acting at its ends and/or to loads acting on it.

Solutions that describe the elastic-plastic in-plane (two-dimensional) behavior of columns and beam-columns comprise the most highly developed aspect of column research in recent years. Applications to practical analysis and design for building frames are quite common, and the basic techniques are given in several texts and codes.

Despite this progress in obtaining solutions for in-plane behavior of columns, their extensions to three-dimensional space situations are just beginning, although some solutions have been obtained. The mathematics of such columns is quite involved, even for the special case of relatively short columns for which the effect of lateral deflections on the magnitudes of bending moments is negligible. For the most part, analysis and design of such columns have in the past been directed toward the study of ultimate strength of reinforced concrete short columns. For the case of long columns, the present design procedure of biaxially loaded columns does not differ from uniaxially loaded columns. The 1971 ACI Building Code, for example, recommends to calculate the moment magnifier separately and apply to the moment about each axis independently. The long columns are then designed according to the given axial compressive load and the magnified biaxial moments.

Although this procedure has been used extensively in design computations, it does not give accurate indications of the true load carrying capacity of a biaxially loaded column. To determine the ultimate strength of such a column, it is necessary to perform an elastic plastic stability analysis that considers the entire range of loading up to ultimate load. In order to perform such an analysis, we must have the knowledge of elastic-plastic behavior of a section under combined axial force, and biaxial bending moments. This is described in the present paper.

In this paper, an elastic-plastic analysis of a reinforced concrete segment under combined axial force, and biaxial bending has been obtained. The segment can be loaded with various combinations of loading path. For example, the section can be loaded first under a constant axial load P , and bending moment M_x , and then P , and M_x held constant while the section is loaded to its fully plastic state by the bending moment M_y . Computer programs have been used to replace the tedious calculations and series of plots which would have to be made to obtain the corresponding generalized strains of the segments at various stages of loading. With the knowledge of this elastic-plastic behavior of a segment under combined axial force, and biaxial bending, this fundamental result has been applied successfully to obtain elastic-plastic long column solutions. Several design criteria for reinforced

concrete columns subjected to compression combined with biaxial bending are developed and reported elsewhere (IABSE Symposium on Design and Safety of Reinforced Concrete Compression Members, Quebec, 1974).

References

1. SANTATHADAPORN, S., and CHEN, W.F.: Tangent Stiffness Method for Biaxial Bending. J. of the Structural Division, ASCE, Vol. 98, No. ST1, January 1972, pp. 153-163.
2. WARNER, R.F.: Biaxial Moment Thrust Curvature Relation. J. of the Structural Division, ASCE, Vol. 95, No. ST5, May 1969, pp. 923-940.
3. ACI Committee 318-71: Building Code Requirements for Reinforced Concrete (ACI 318-71). American Concrete Institute, Detroit, 1971.
4. BRESLER, B.: Design Criteria for Reinforced Columns under Axial Load and Biaxial Bending. J. of the American Concrete Institute, v. 32, No. 5, November 1960.

Summary

An analytical formulation of the force-deformation equations in terms of the increments has been developed which enables one to obtain the complete moment curvature relationships of a short reinforced concrete column, subjected to axial load and biaxial bending moments, at all load levels. The method is found to be extremely powerful and efficient for computer solution.

The computer program based on this formulation can be integrated into the long column analysis or into overall structural analysis programs, and is probably very useful and essential in such a study.

Résumé

On développe une formulation analytique des équations force/déformation en termes de l'accroissement permettant d'obtenir les relations complètes de moment/courbure d'une courte colonne en béton armé soumise à une charge axiale et à des moments de flexion biaxiaux pour tous les degrés de charges. La méthode est extrêmement efficace pour la solution par ordinateur. Le programme d'ordinateur basé sur cette formulation peut être intégré dans l'analyse de colonnes longues ou dans tous les programmes d'analyse structurale et s'avérera probablement très utile.

Zusammenfassung

Es wird eine rechnerische Formulierung der Kraft/Deformations-Gleichungen in Termen des Zuwachses entwickelt, die es gestattet, die vollständige Moment/Krümmungsbeziehung einer kurzen Stahlbetonstütze unter Einfluss axialer Belastungsstufen zu erfassen. Die Methode erwies sich als äusserst wirksam und

brauchbar für eine Lösung mittels Computer. Das auf der Formulierung beruhende Computerprogramm lässt sich entweder auf die Berechnung für lange Stützen oder auf alle baulichen Rechenprogramme anwenden und erweist sich voraussichtlich als ebenso nützlich wie wesentlich.